NANO MICRO small

Self-Assembly

Optically Controlled Pore Formation in Self-Sealing Giant Porphyrin Vesicles

*Elizabeth Huynh, Jonathan F. Lovell, Ryan Fobel, and Gang Zheng**

***E**fforts to develop self-contained microreactors and artificial cells have been limited by difficulty in generating membranes that can be robustly and repeatedly manipulated to load and release cargo from phospholipid compartments. Here we describe a purely optical method to form pores in a membrane generated from porphyrin-phospholipid conjugates electro-assembled into microscale giant porphyrin vesicles and manipulated using confocal microscopy. The pores in the membrane resealed within a minute allowing for repeated pore formation with precise spatial and temporal control and optical gating to allow selective diffusion of biomolecules across the membrane. Temporal control of pore formation was illustrated by performing sequential DNA hybridization reactions. A biotin-avidin based strategy was developed to selectively attach enzymes to the interior of the vesicle, demonstrating spatial control and the potential of giant porphyrin vesicles as versatile microreactors.*

1. Introduction

Phospholipid-enclosed compartments play a central role in cellular and sub-cellular homeostasis, with the bilayer serving as the general barrier between external and internal biomolecules and chemicals. Putative prebiotic bilayers have been recreated in the context of understanding and mimicking how cells came to control the passage and production of biomolecules.[1] A wide range of protein-based transport systems have evolved in organisms to permit the movement of molecules through bilayers without destroying the overall membrane integrity. However, these transport systems are typically specific for certain cargo and are not suitable as general-purpose gateways to the interior of natural or synthetic phospholipid-enclosed compartments. Thus, disruptive techniques such as, electroporation and heat shock have been developed to permit the passage of biomolecules, such as DNA, through cell membranes.[2] While highly practical for some applications, the positioning and timing of pore formation using these methods are not easy to control. The pore formation and resealing of swollen, giant lipid vesicles have been well characterized, but again, the process is not readily controllable and has traditionally made use of highly viscous solvents that preclude many applications.[3] More precise control of bilayer permeability has been achieved using novel approaches such as local electroporation,[4] proximal heating of gold nanoparticles,[5] electroinjection[6] and photoporation,[7–9] many of which involve the addition of an exogenous agent or highly sophisticated instruments.

Here we describe a simple optical technique to robustly control membrane permeability in a cell-sized vesicle based on the unique properties of a porphyrin-lipid bilayer and widely available confocal microscopy. The porphyrin-lipid bilayer mimics a biological cell's response to light by forming

E. Huynh, Prof. G. Zheng
Ontario Cancer Institute and Techna Institute
University Health Network
Toronto, Ontario M5G1L7, Canada
Department of Medical Biophysics
University of Toronto
Ontario, M5G1L7, Canada
E-mail: gzheng@uhnresearch.ca
Dr. J. F. Lovell
Department of Biomedical Engineering
University at Buffalo
State University of New York
NY, 14260, USA
R. Fobel, Prof. G. Zheng
Institute for Biomaterials and Biomedical Engineering
University of Toronto
Ontario, M5G1L7, Canada

DOI: 10.1002/smll.201302424

a transient pore upon laser irradiation, which then proceeds to self-seal. We draw parallels between this method on artificial cells and photoporation on biological cells through DNA transfection and further extend the unique control of this method for use in low-volume reactions. The discovery of light responsive membranes has broad implications for the development of protocells and microreactor applications.

2. Results and Discussion

We recently reported that porphyrin-lipid conjugates could self-assemble into liposome-like nanovesicles formed from a porphyrin bilayer.[10] To examine whether larger micron-sized porphyrin vesicles could be formed, we developed a modified electroformation approach, based on the alternating current method.[11] Using a low cost, open-source programmable Arduino microcontroller, a solution of varying fractions of porphyrin-lipid (pyropheophorbide-lipid) (**Figure 1**a I) and egg phosphatidylcholine with cholesterol in chloroform was coated onto platinum wires, evaporated, rehydrated and subjected to a low-frequency alternating square wave field (Figure 1a II, see supporting materials for the commented Arduino code and more detailed circuit diagram). Using this method, micron-scale vesicles were readily generated and could be visualized using confocal microscopy (Figure 1a II, inset). Pyrophoephorbide (pyro) was chosen as the porphyrin for the lipid-conjugate as the characteristic optical absorption spectral properties (Figure S1) allowed both manipulation by high intensity light (using a 405 nm laser) and imaging of the response to irradiation (using a 633 nm laser) by confocal microscopy since pyro absorbs strongly at both these wavelengths. In the presence of the electric field, vesicles formed spontaneously and slowly detached from the platinum wires, and this process continued repeatedly over time. Removal of the electric field prevented the oscillations necessary for the vesicle detachment, leaving a high density of relatively immobilized giant porphyrin vesicles (GPVs) proximal to the wires which greatly facilitated time-series observation by confocal microscopy. Because the porphyrin component of the lipid conjugate, pyropheophorbide (pyro), is fluorescent, the bilayer could be imaged using fluorescence microscopy without any exogenous label. We examined how increasing proportions of porphyrin-lipid affected two types of movement-restricted vesicles: detached, sucrose-containing vesicles that sank when transferred to a separate solution of lesser density glucose, and vesicles immobilized on the platinum wire. In both cases, spherical vesicles 10–50 μm in size were formed, and the addition of greater than 1 molar% porphyrin-lipid led to fluorescence self-quenching of the entire vesicle due to the higher porphyrin content (Figure 1b). The consistent porphyrin depth within the bilayer held in place by the amphipathic nature of the porphyrin-lipid, combined with the high porphyrin density suggest that the bilayer environment created dynamic face to face porphyrin interactions, leading to fluorescence quenching. However, microvesicle yield and circular geometry quality decreased beyond 70 molar% porphyrin-lipid, demonstrating that some standard phospholipids were helpful to form the GPVs.

Each 10 μm porphyrin vesicle formed from 70 molar% porphyrin-lipid was estimated to contain approximately 6×10^8 porphyrins, all confined to the thin, enclosing porphyrin bilayer. Given the high optical absorption of the porphyrin bilayer, the membrane response to laser irradiation was investigated. Despite the high level of fluorescence self-quenching (75% quenched compared to 1% pyro-lipid giant vesicles), the bilayer retained enough fluorescence to enable clear optical observation of the bilayer response using a 633 nm laser to excite the Q-band of pyro. Confocal microscopy is commonly used to study the fluorescence recovery after photobleaching (FRAP) of a cell membrane induced by a focused laser incorporated into the microscope set-up.[12] We applied this focused laser pulse with a wavelength of 405 nm to the GPV membrane, which directly excited the more intense pyro Soret band. The laser power was estimated to be 660 μW and was focused into a small area to achieve a laser fluence rate on the order of kWs per cm^2. When the bilayer was subjected to a 200 ms pulse confined to a 2 μm diameter spot on the membrane (a high laser fluence of 42 $\mu J/\mu m^2$; intensity: 210 $\mu W/\mu m^2$), the bilayer was observed to form a large micron sized pore, 10–15 μm in diameter in the membrane of a 30 μm diameter GPV for an extended period of time (Figure 1c and Supplementary Movie M1). After 30 seconds, the membrane edges of the pore came together, resealed and the vesicle appeared intact again, returning to its original state. Although they displayed less contrast, phase contrast images confirmed that the bilayer was physically forming a large pore and resealing, as opposed to a local fluorescence bleaching of the bilayer. Single slice images were taken through the volume of the GPV and reconstructed to provide a 3D rendering of the vesicle before and after laser irradiation, demonstrating that upon laser irradiation a large micron sized pore formed through the bilayer and extended in all directions (Figure 1d and Supplementary Movie M2).

Having observed this pore formation and resealing behaviour of GPVs formed from 70% porphyrin-lipid, repeated pore formation and self-sealing of GPVs was investigated and compared with the behaviour of vesicles formed from 1% porphyrin-lipid. As shown in **Figure 2**a, a GPV formed from 70% porphyrin-lipid could repeatedly form large pores and self-seal indefinitely. However, when 1% porphyrin-lipid was incorporated into the bilayer, no membrane opening was observed after applying the same high laser fluence (42 $\mu J/\mu m^2$; intensity: 210 $\mu W/\mu m^2$). Various GPV responses to laser irradiation were categorized as no response, membrane stretching, opening alone (pore formation), or opening and closing (pore formation and resealing) (see Figure S2 for an example of membrane stretching). None of the varying laser powers examined (fluence range: 4 $\mu J/\mu m^2$ to 42 $\mu J/\mu m^2$; intensity: 21 $\mu W/\mu m^2$ to 210 $\mu W/\mu m^2$ irradiated for 200ms) could induce pore formation in the highly fluorescent 1% porphyrin-lipid microvesicles (Figure 2b). However, pore formation and resealing was observed consistently for the 70% porphyrin-lipid GPVs, with the percentage of opening and closing events increasing with greater laser power. A small subset of GPVs remained open and did not reseal even after several minutes. A similar trend was observed as the irradiation area was increased from 2 μm to 12 μm, effectively

small 2013,
DOI: 10.1002/smll.201302424

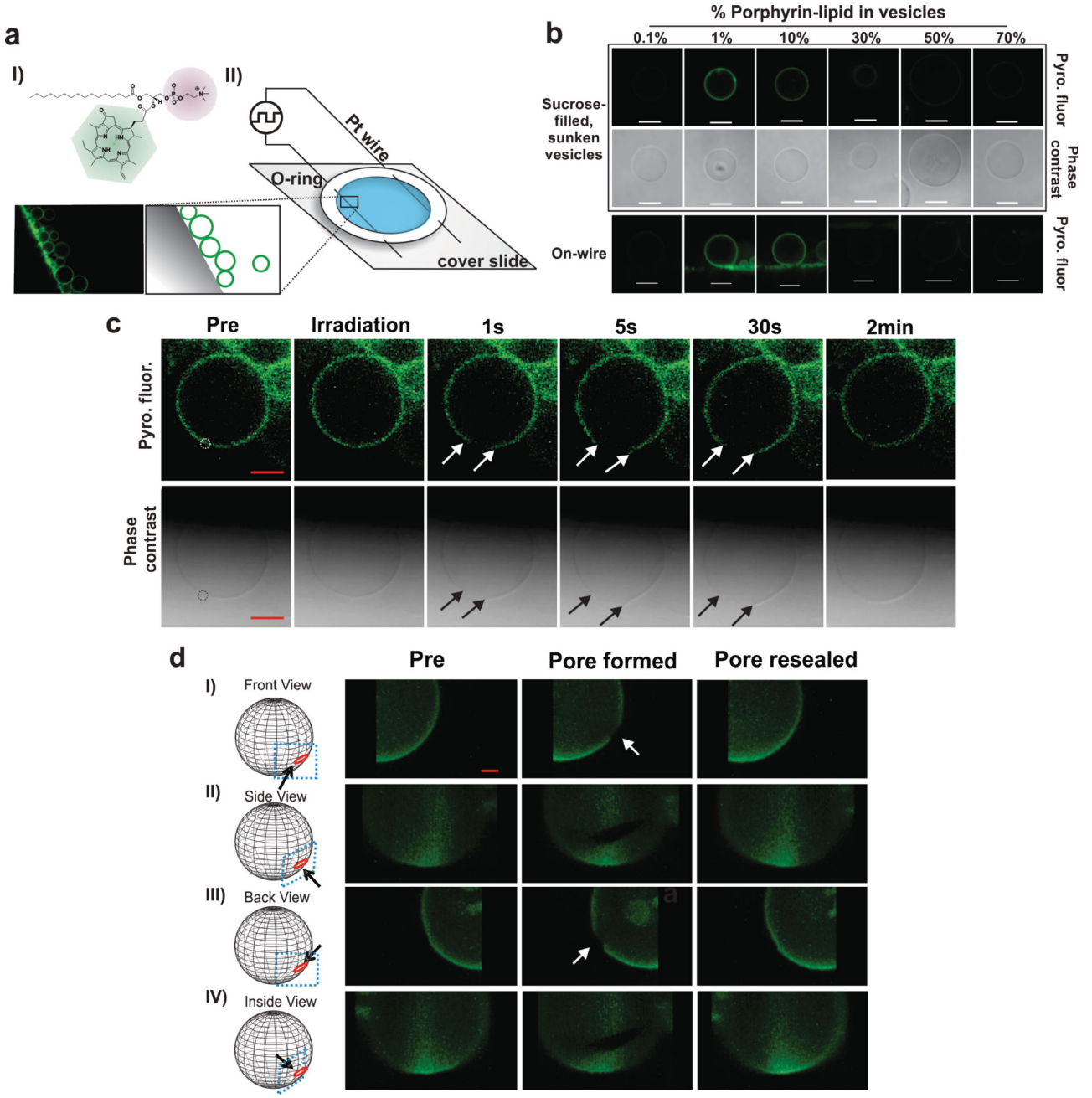

Figure 1. Generation and pore formation in giant porphyrin vesicles (GPVs). (a) I) Schematic of porphyrin-lipid used to form GPVs; II) Experimental setup used for GPV electroformation using a microcontroller to generate an AC field. The apparatus set up is shown on the right. The left insets show a confocal micrograph (left) and a schematic image (right) of GPVs formed on the wire. (b) Fluorescence quenching of GPVs formed in two different environments: 1) encapsulating sucrose and dispersed in glucose, or 2) immobilized on the platinum wire. Fluorescence settings were the same in each image. 10 µm scale bar is shown. (c) GPVs containing 70% pyro-lipid formed a pore upon laser irradiation (white dashed circle) and then self-sealed. Arrows show GPV pore. 10 µm scale bar is indicated. (d) 3D image of a GPV reconstructed from z-stack slices. Schematic representation of a GPV (left) indicating the section of the vesicle imaged (blue dashed box), pore region (red circle) and the point of view (black arrow) corresponding to pre-irradiation, pore formation and after resealing images (right). White arrow indicates pore. 5 µm scale bar is indicated.

decreasing the laser fluence from 42 µJ/µm^2 (intensity: 210 µW/µm^2) to 1 µJ/µm^2 (intensity: 6 µW/µm^2), respectively (Figure 2c).

A substantial amount of experimental and theoretical work has led to an understanding of pressure-induced opening and closing of conventional giant unilamellar vesicles (GUVs).[13–15] In these well-established models, pore formation is initiated and propagated by increased surface tension. Once the pore forms, lipids re-orient themselves to minimize hydrophobic side-chain exposure to the aqueous environment, but this modified packing structure has a free energy cost. Thus, an edge tension force is generated that opposes pore formation and is responsible for pore closure. Pore dynamics are balanced by the opposing forces of edge

DOI: 10.1002/smll.201302424

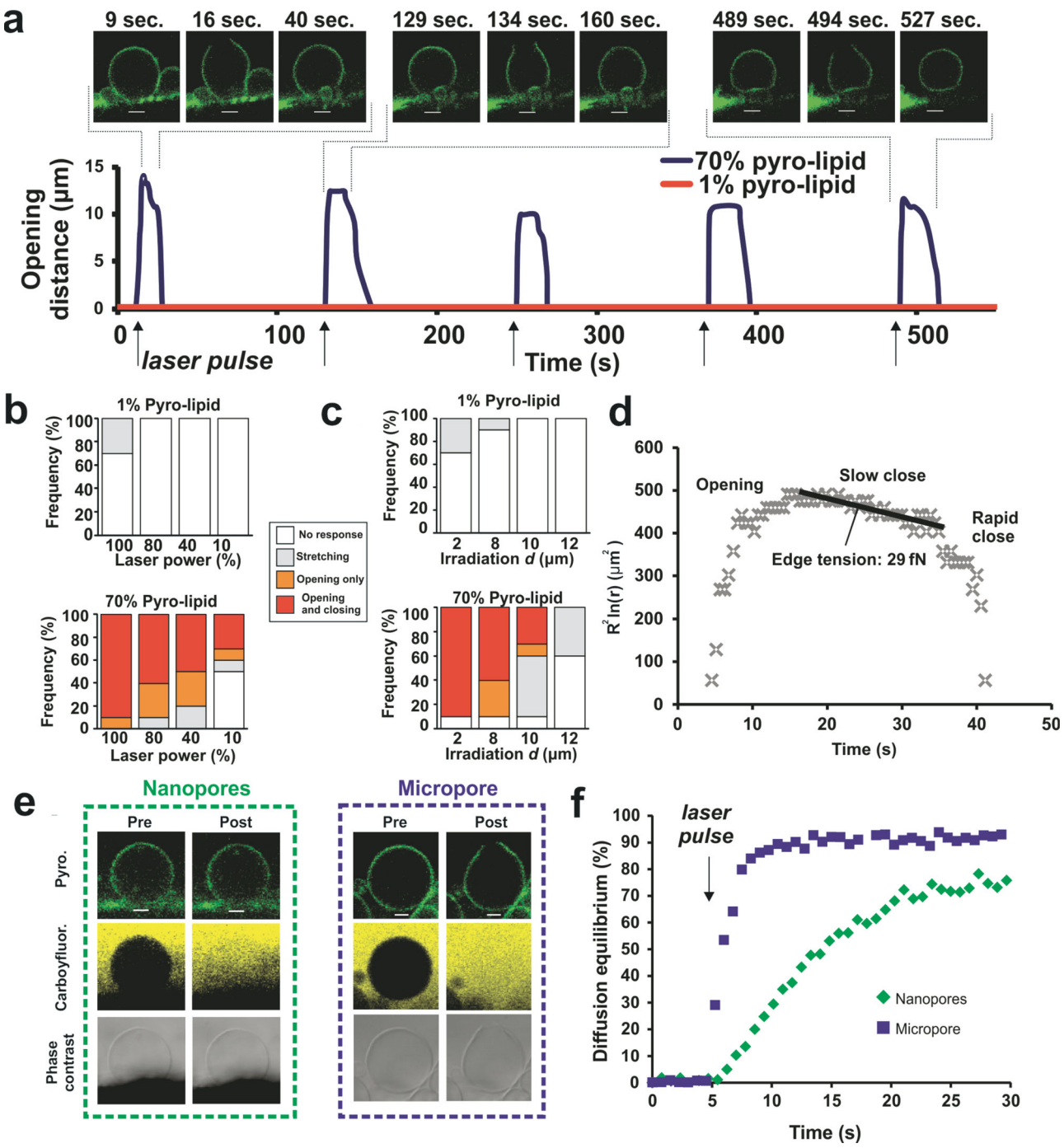

Figure 2. GPV pore formation and self-sealing. (a) Repeated pore formation and self-sealing of a GPV. Arrows indicate time of laser pulsing (laser fluence: 40 μJ/μm^2). (b) GPV response to laser irradiation with varying laser power and (c) irradiation spot diameter using a 200 ms irradiation time. Frequency charts are based on results from 10 separate GPVs irradiations per bar. (d) Estimation of edge tension force in GPV pores. A typical pore opening is shown, plotted as $R^2\ln(r)$ as a function of time, where R is the GPV radius and r is the pore radius. The edge tension during the slow close period, based on the slope of the black line (slope = −6.75 ± 1.51, n = 3 ± standard error), was 29 ± 7 fN. Laser fluence: 40 μJ/μm^2. (e) Types of pores formed by GPVs. Low laser fluences (1 μJ/μm^2) produce nanopores whereas high laser fluences (40 μJ/μm^2) produce micropores, both allowing the diffusion of carboxyfluorescein (0.4kDa). 5 μm scale bar shown. (f) Diffusion equilibrium of carboxyfluorescein into GPVs through different pore types.

tension and surface tension. We hypothesize that in the case of GPVs, the porphyrin bilayer may stabilize the pore edge and reduce the edge tension force. As shown in Figure 2d, a typical GPV opening followed conventional patterns of lipid vesicle opening, with a rapid opening, slow closing and fast closing phase. Based on mathematical models developed by the Brochard-Wyart group[13] and recently further elucidated by the Dimova group,[15] it has been demonstrated that the edge tension can be calculated during the slow closure period from the slope of $R^2\ln(r)$ as a function of time, where R is the

small 2013,
DOI: 10.1002/smll.201302424

NANO MICRO small

radius of the GUV and r is the radius of the pore.[13,15] The edge tension, γ, can then be calculated from Equation (1):

$$\gamma = -(3/2)\pi\eta a \quad (1)$$

a represents the slope of the linear fit of the slow closure phase shown in Figure 2d and η is the viscosity of the medium, water in this case (8.9×10^{-4} Pa s). Using this technique, we estimate a typical edge tension force during GPV closing of 29 ± 7 fN. This value is noteworthy as it is approximately 3 orders of magnitude smaller than conventional phospholipid bilayers.[15] Thus, the edge of the porated porphyrin bilayer appears to be significantly stabilized by the porphyrin itself. This may be from the extensive and dynamic face to face porphyrin pi-pi electron interactions that occur in the GPV bilayer.

In order to examine whether small molecules could diffuse through the porated membrane and the effect of varying the laser fluence, carboxyfluorescein was added to the exterior of the GPV. No fluorescence was observed inside the GPVs following addition of the fluorophores into the solution, demonstrating that the porphyrin bilayer was impermeable to these molecules. GPVs were irradiated with high and low laser fluences using 42 μJ/μm^2 (intensity: 210 μW/μm^2) for high laser fluence and 1 μJ/μm^2 (intensity: 6 μW/μm^2) for low laser fluence, unless otherwise indicated. When the GPVs were irradiated with a high laser fluence (40 μJ/μm^2), carboxyfluorescein freely diffused into the GPV within seconds and the edges of the GPV membrane was seen to physically come apart and form a micron sized pore, verified by the phase contrast image (Figure 2e and f). When GPVs were irradiated with a low laser fluence (1 μJ/μm^2), carboxyfluorescein also diffused into the GPV but at a much slower rate, indicating the presence of small pores that limited the rate but did not restrict molecule diffusion (Figure S3). Furthermore, the membrane of the GPV was not observed to form a large micron sized pore as with the higher laser fluence, suggesting that nanopores could form in the membrane under low laser fluence but were not visible due to the resolution limitations of the microscope. Therefore, two types of pores can be formed in the GPV membrane: nanopores using low laser fluence and a micropore using high laser fluence.

The formation of these pores in the GPV membrane were dependent upon two factors: laser fluence and porphyrin-lipid concentration, as vesicles formed from 1% porphyrin-lipid did not exhibit the ability to form visible pores or allow the diffusion of carboxyfluorescein using either the high or low laser fluence (Figure S4) and in GPVs formed from 70% porphyrin-lipid, laser fluences less than 0.5 μJ/μm^2 did not induce pore formation (Figure S5). Porphyrin fluorescence self-quenching has been shown to be highly correlated with self-quenching of singlet oxygen quantum yield.[16] Although less quenched, 1% porphyrin-lipid GPVs generated substantially more fluorescence and thus more singlet oxygen (hundreds of fold more, based on the quenching in porphysomes of similar composition[10]), they did not form pores in response to laser irradiation, indicating that pore formation is not a result of singlet oxygen interaction with the membrane. This is consistent with previous examination of singlet oxygen generation of porphyrins anchored in low molar percentages (1–10%) in phospholipid giant unilamellar vesicles, which did not produce visible membrane poration in response to irradiation.[17] Furthermore, destabilization of membranes based on singlet oxygen production occurs by reduction of phospholipid tails when unsaturated bonds interact with singlet oxygen.[17,18] When GPVs were formed with 30% 1,2-dipalmitoyl-sn-glycero-3-phosphocholine (DPPC), a saturated lipid, in place of egg PC that contains 1-palmitoyl-2-oleoyl-sn-glycero-3-phosphocholine (POPC), an unsaturated lipid, pore formation was still consistently observed. In addition, when GPVs were formed with different transition temperature lipids, while applying the same laser parameters, increasing the transition temperature of the lipid resulted in a slower efflux of fluorophore out of the GPV (Figure S6). We hypothesize that the formation of these pores observed in GPVs are induced by a thermal mechanism. We previously demonstrated that nanoparticles formed from porphyrin-lipid possessed intrinsic biophotonic properties, rivalling gold nanoparticles, due to extreme fluorescence self-quenching resulting in high heat generation.[10] Gold nanoparticles are known to provide efficient conversion of optical energy into thermal energy. Furthermore, under high laser fluence, gold nanoparticles generate vapor bubbles around the nanoparticle due to rapid heating and vaporization of the surrounding medium.[19,20] The dependence of pore formation in GPVs on high porphyrin content (resulting in fluorescence self-quenching (Figure 1b), and high laser fluence indicate that pore formation may be due to high heat generation. For nanopores, irradiation with low laser fluence causes thermal heating of the membrane, resulting in an increase in membrane fluidity, which allows small molecules to permeate the membrane. However, upon irradiation using high laser fluence, rapid local heating may result in the formation of transient vapor bubbles which rapidly increases the membrane tension near at the pore site, forcing the edges of the membrane apart, resulting in the formation of a micron sized pore, much larger than the irradiation spot size (Figure 1c and d). Vapor bubbles generated by gold nanoparticles are known to have a life time on the scale of nanoseconds,[19] which is beyond the temporal resolution of the confocal microscope and could not be directly observed in GPVs. Further work is required to fully elucidate and model the mechanism and physics of GPV pore formation and resealing, but it is likely due to a photophysical process which results in the production of thermal energy which increases the membrane tension near the pore site.

The ability to form two types of pores in GPVs permits a plethora of possible applications as an artificial cell or microreactor. The micropore allows the encapsulation of large particles such as microparticles, cells or bacteria, whereas the nanopores allow for the loading and release of smaller cargo such as chemical reactants. Furthermore, the rate of diffusion of biomolecules through micropores is proportional to the size of the molecule. We quantified the internalization rate of three fluorophores of varying sizes through micropores and observed that the smaller 0.4 kDa carboxyfluorescein diffused in faster than the 10 kDa Texas Red dextran, which in turn diffused faster than the 155 kDa TRITC dextran

DOI: 10.1002/smll.201302424

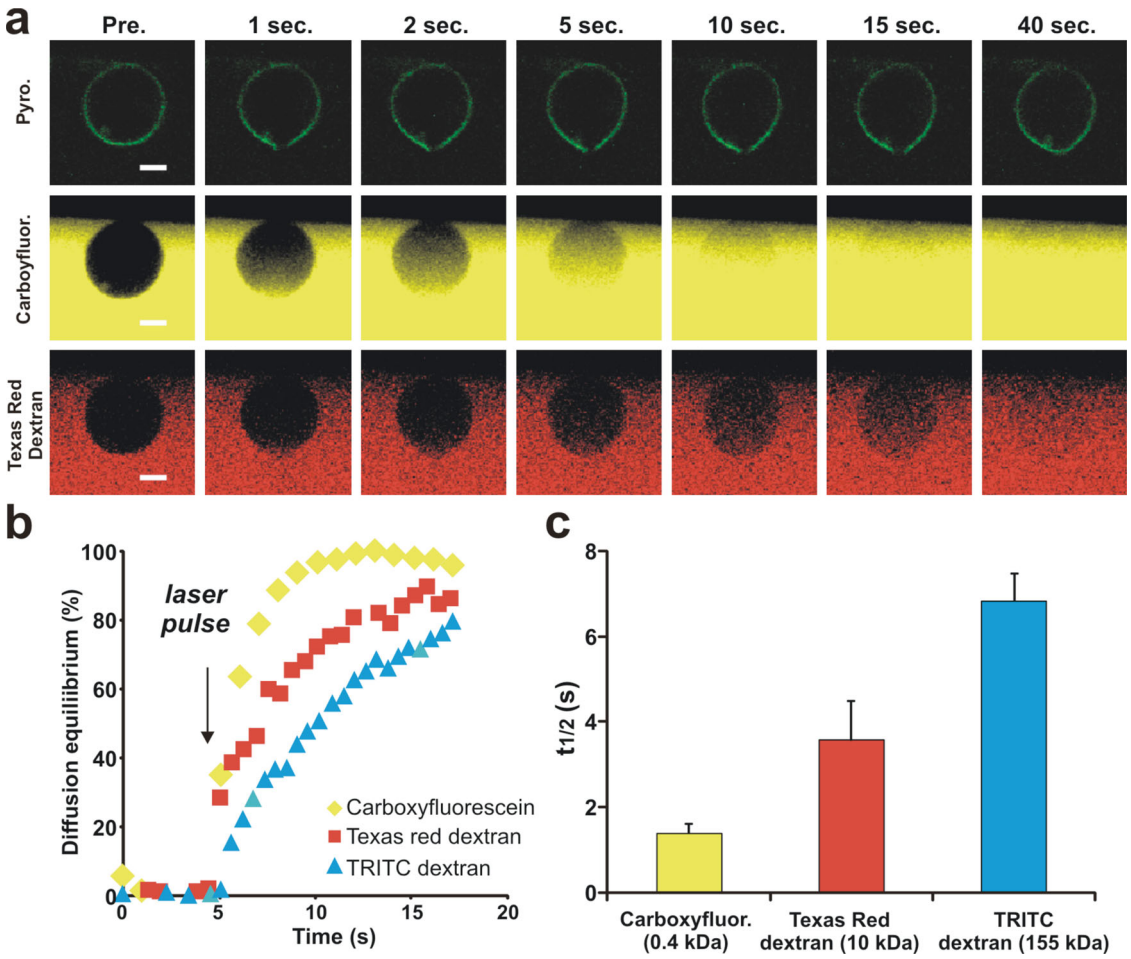

Figure 3. Diffusion of biomolecules into GPVs through a micropore. (a) Confocal images of GPVs and exogenous fluorophores added to the solution before and after laser irradiation (laser fluence: 40 μJ/μm^2). 10 μm scale bar is shown. (b) Diffusion equilibrium of various fluorophores into GPVs. (c) Half-times to diffusion equilibrium for various sized fluorophores (mean + /– SD from 5 separate GPV irradiations per fluorophore).

(**Figure 3**a and b). The time required for half the molecules to diffuse into the GPVs following opening varied from 1 to 8 seconds based on the size of the cargo (Figure 3c) as would be expected for smaller molecules, which diffuse more rapidly. Nanopores enable user-controlled loading or release of size dependent cargo. To demonstrate the release of cargo from GPVs, GPVs were formed in the presence of two fluorophores, carboxyfluorescein (0.4 kDa) and TRITC dextran (155 kDa). The exterior medium was replaced in order to wash away free fluorophore. Using a low laser fluence (2 μJ/μm^2; intensity: 10 μW/μm^2), low molecular weight cargo (carboxyfluorescein, 0.4 kDa) could be released through nanopores, while retaining larger molecular weight cargo (TRITC dextran, 155 kDa) (**Figure 4**a and b). Applying a higher laser fluence (20 μJ/μm^2; intensity: 33 μW/μm^2) enabled the release of the larger cargo (Figure 4c and d), indicating the presence of larger pores. The dependence of pore size on laser fluence, especially with nanopores, provides a means of optical gating with the user having the ability to control the precise loading/release of specific cargo. This method of optical gating is especially important in microreactor applications, allowing multistep reactions with the loading of specific reactants without releasing products generated from previous steps and without the use of exogenous agents, not previously possible with other injection techniques used for vesicle compartments.

As photoporation techniques are frequently used for gene transfection into cells, to demonstrate that a GPV could be repeatedly optically manipulated with precise timing and allow the encapsulation of DNA into an artificial cell-like membrane, laser induced membrane pore formation was used to control the passage of oligonucleotides (**Figure 5**). When a fluorescein-labeled DNA oligonucleotide was incubated with preformed GPVs, it remained outside the vesicles. Upon laser-induced opening (fluence: 42 μJ/μm^2; intensity: 210 μW/μm^2), the DNA diffused into the GPV, as indicated by an increase in internalized fluorescence. Next, a complementary strand labeled with dabcyl, a dark quencher, was added to the external buffer. The fluorescence of the solution was markedly attenuated. However, the interior of the GPV remained fluorescent, as the quenching oligonucleotide could not pass the porphyrin bilayer to reach the DNA that had been encapsulated. Finally, when the GPV was opened again, the quencher and

small 2013,
DOI: 10.1002/smll.201302424

NANO MICRO small

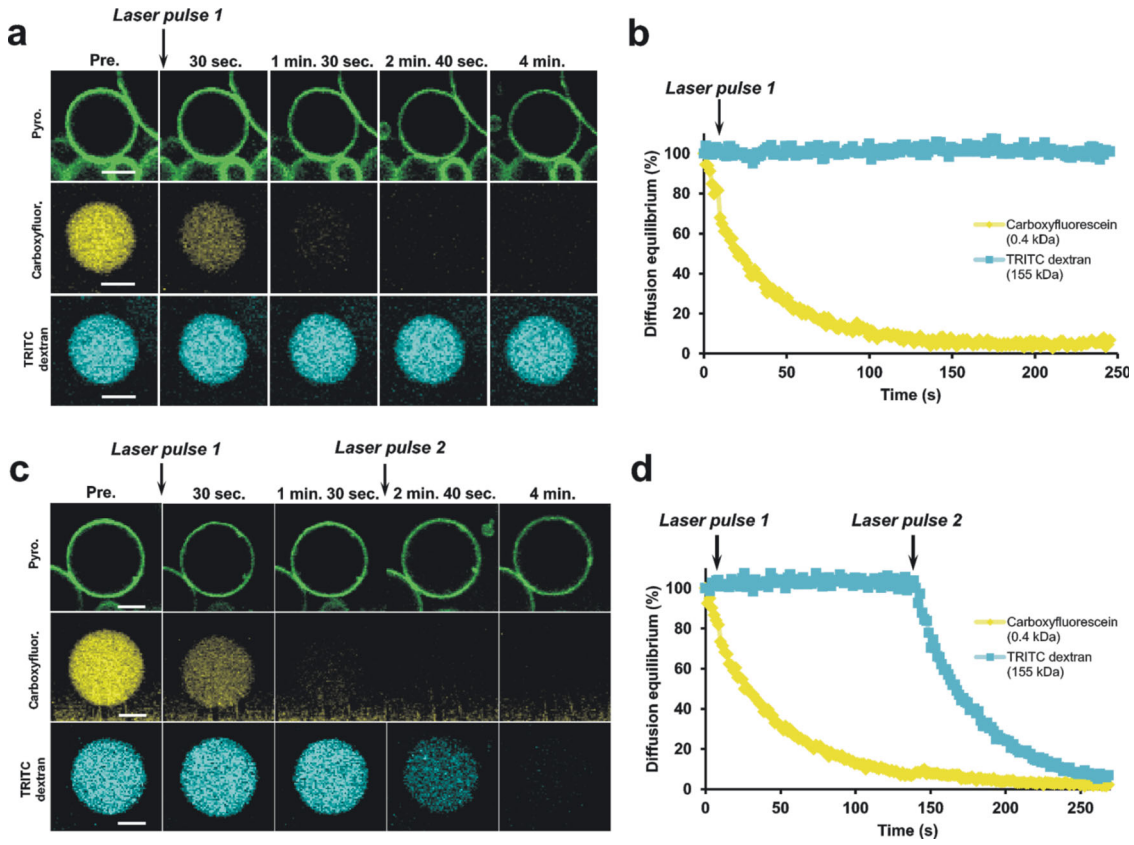

Figure 4. Size dependent optical gating of cargo. Different molecular weight fluorophores, carboxyfluorescein (0.4 kDa) and TRITC dextran (155 kDa), were co-encapsulated in GPVs and external fluorophores were removed by washing. (a,b) A GPV was irradiated with a pulse of low laser fluence (laser pulse 1: 2 μJ/μm^2) and low molecular weight molecules (carboxyfluorescein) were released; however the larger fluorophores (TRITC dextran) remained trapped inside the GPV. 10 μm scale bar shown. (c, d) A GPV was first irradiated with a pulse of low laser fluence (laser pulse 1: 2 μJ/μm^2) and carboxyfluorescein was released while TRITC dextran remained inside. After 2 minutes, a second pulse of greater laser fluence (laser pulse 2: 20 μJ/μm^2) was applied and the large TRITC dextran was released. 10 μm scale bar shown.

quenched hybridized DNA could diffuse into the interior and eliminate the fluorescence coming from the GPV. The timing of pore formation in the GPV was precisely controlled between addition of the oligonucleotides and closing of the membrane. This illustrates the temporal control associated with this method, which is essential for sequential reactions, and the ability to transfect GPVs with DNA, a common application of photoporation.

The ability to predetermine the location of pore formation and induce a pore at a specific time point is a highly advantageous characteristic that many membrane permeability techniques lack. In addition, a useful enclosed microreactor should also confine the desired reaction to the interior space of the vesicle. We developed a strategy to selectively attach enzymatic molecules of interest to specific locations within the interior of GPVs (**Figure 6**a). By including a small molar percentage of biotinylated lipid in the formulation, GPVs could be formed that were prone to avidin binding, which is essentially an irreversible association with biotin in standard aqueous conditions. The exterior of the GPVs were blocked with a 2 fold molar excess of avidin, ensuring all biotin sites on the exterior leaflet of the GPV bilayer were occupied. A 4 fold excess of fluorescein labeled avidin was then added to the external medium. The single pores were formed in preselected regions of the GPV membrane using laser irradiation (fluence: 42 μJ/μm^2; intensity: 210 μW/μm^2). The labeled avidin did not freely diffuse into the GPV and bind uniformly around the circumference. Instead, it bound exclusively around the pore site inside the GPV (Figure 6b). This may be due to the smaller opening that was induced in the membrane when the biotin and avidin was used. This process was repeated 8 times to illustrate the spatial control of this method and achieve uniform spacing of labeled avidin around the periphery of the GPV interior. In this case, we used fluorescently labeled avidin, but enzyme-avidin conjugates are also available and could be placed in the GPV interior in the same manner. Eventually, following selective enzyme attachment to the GPV interior, substrates could be diffused into the GPVs to become enzymatically transformed into products and then released on demand by porphyrin bilayer pore formation. This approach could prove useful for small volume reactions for enzyme activity optimization, screening approaches or sequential reactions. In addition, as several reactions and biological processes are observed in physiological conditions, GPVs could also be formed in physiological salt conditions and demonstrate the same pore

DOI: 10.1002/smll.201302424

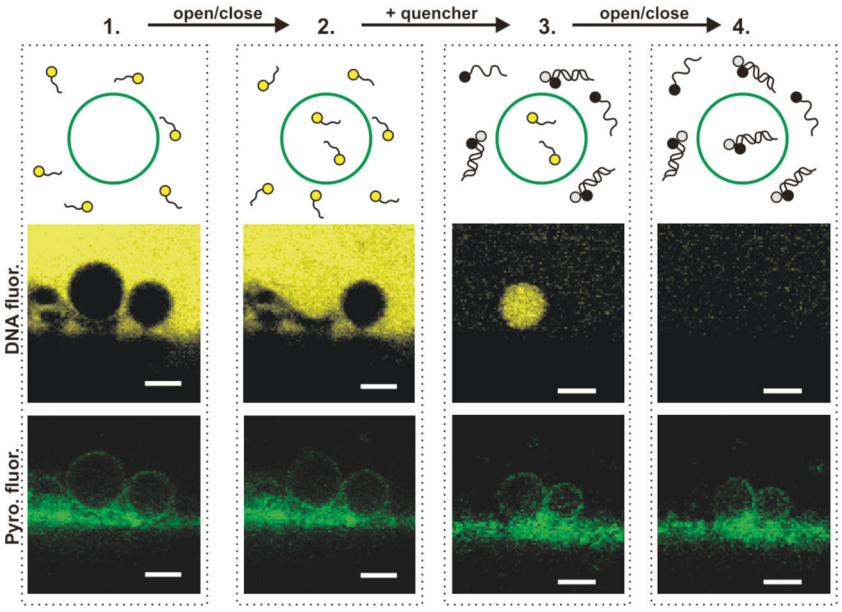

Figure 5. Temporal control illustrated using sequential DNA hybridization in GPVs. Fluorescently labeled DNA exterior of the GPVs (1, yellow) was permitted to enter the left GPV following laser opening (2) (laser fluence: 40 μJ/μm^2) whereas the right GPV remained empty. A complementary sequence with a quenching moiety was then added to the external medium attenuating the external fluorescence outside the GPVs (3) and again the left GPV was opened (laser fluence: 40 μJ/μm^2) to allow the quenching to occur inside the GPV (4). 10 μm scale bar is shown.

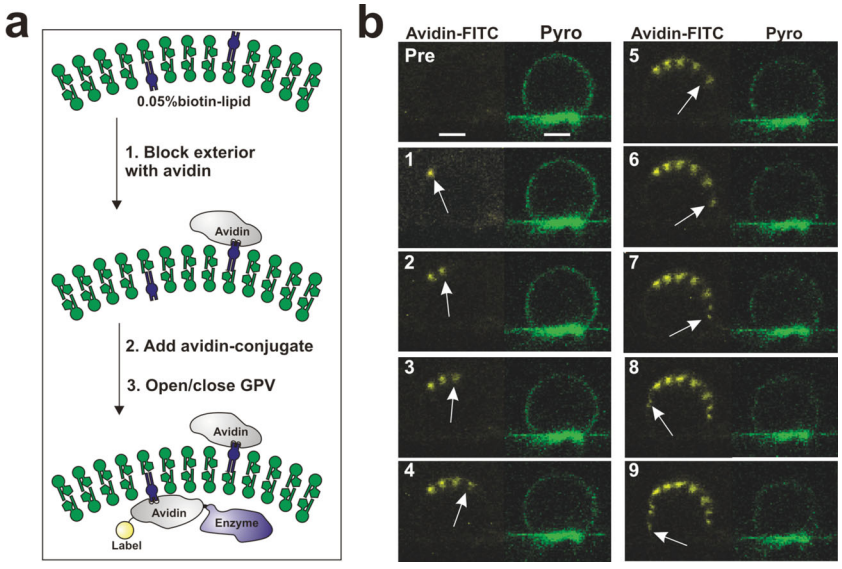

Figure 6. Spatial control and a strategy for selective attachment of enzymes to the interior of the GPV. (a) Schematic representation of blocking the external leaflet biotin sites using avidin, followed by addition of an avidin-conjugate, and opening and closing of the GPV to selectively place the avidin conjugate (which could be labeled with a fluorophore or attached to another enzyme) inside the GPV. (b) Multiple pore formation and resealing events can evenly distribute the avidin-conjugates of interest inside GPVs. Following exterior blocking, FITC-avidin was placed in the medium and the GPVs were opened and closed multiple times in the order the numbering indicates (laser fluence of 40 μJ/μm^2). 10 μm scale bar shown. Cell-sized porphyrin vesicles are able to respond to light with precise control over timing, location and size of pore formation. These unique properties based on a porphyrin-lipid bilayer are useful microreactors and can be applied in protocell development.

formation behaviour by simply increasing the parameters of the electric field used for electroformation and laser irradiation (Figure S7).

In photoporation, ultraviolet femtosecond lasers are often used to generate highly localized transient pores in cells in a sterile environment for a number of applications, including gene transfection.[7–9] The formation of these pores are a result of non-linear absorption in biological molecules such as membrane proteins, that create electron plasmas which induce thermal, chemical and thermomechanical effects.[21] Photoporation is an attractive option for loading of cargo as it is a purely optical, repeatable and sterile method with precise control over pore formation, all of which are characteristics that other methods lack. To our knowledge, femtosecond laser photoporation has been restricted to applications directly involving cells and has not been applied with artificial cells composed of phospholipid membranes, as phospholipids do not absorb in the ultraviolet range. Continuous wave lasers have also been employed for photoporation, especially for membrane permeabilization applications in cells.[22] However, this requires staining of the cell membrane with a dye[23] or the use of high output laser powers (>1W)[24] as the use of continuous wave lasers for photoporation is based on linear absorption.[21] To date, photoporation techniques require instruments not commonly available in biological research settings. Cell-sized phospholipid compartments have been generated in the presence of dyes or membrane-anchored dyes and have observed vesicle bursting[25] or destabilization[17] upon laser irradiation. However, they have not demonstrated advantageous spatially selective membrane poration or precise optical gating of cargo.

3. Conclusion

Here we have described a purely optical technique for the formation of pores in a porphyrin-lipid bilayer possessing unique control characteristics over the timing and spatial region of pore formation as well as the ability to selectively choose the cargo to load or release. This extends the advantages of photoporation to microreactor applications without the use of highly sophisticated lasers and equipment but

small 2013,
DOI: 10.1002/smll.201302424

using widely available confocal microscopy. The laser induced pore formation and self-sealing behavior of GPVs overcomes the limitations involving a lack of control and precision with other techniques used to induce membrane permeability currently associated with synthetic phospholipid compartments while maintaining a sterile environment. In addition, the porphyrin bilayer provides an additional cell-mimicking characteristic to giant vesicles in their ability to robustly and repeatedly respond to laser irradiation and proceed to self-seal, and thus, another step forward towards the generation of a true protocell. The ability to robustly form pores that self-seal has broad reaching consequences and porphyrin bilayers enable programmable vesicle opening and closing.

4. Experimental Section

All chemical materials were obtained from Sigma and electronic materials were obtained from Mouser, unless indicated otherwise. GPVs were formed using a modified electroformation method.[11] Pyropheophorbide-lipid (prepared as previously described,[10] but with a modified protocol to generate an isomerically pure conjugate[26]) in combination with egg phosphatidylcholine (egg PC) and cholesterol (chol) (3:2 molar ratio egg PC: chol) (Avanti Polar lipids), was dispersed in chloroform to form 0.1 mg/ml-0.5 mg/ml stock solutions. Two 0.5 mm diameter platinum wires (#267228, Sigma) were positioned in parallel separated by a distance of 2mm through a small polytetrafluoroethylene O-ring (#9559K208, McMaster-Carr) adhered to a cover slide using vacuum grease. 6–10 equally spaced 1 µl droplets of stock solution were deposited on the two platinum wires. Unless otherwise noted 70 molar% pyropheophorbide-lipid was used. Residual chloroform was evaporated by placing the O-ring apparatus in a vacuum for 20 minutes. A 0.6 mL water solution with 2 mM Tris pH 8 was then used to hydrate the lipids on the wire. The apparatus was connected to a 3V, 10 Hz AC current in order to induce electroformation of the vesicles. A low cost, open source Arduino microcontroller was used to generate the field as per the circuit diagram and the code in the supporting materials section. Vesicles formed on the wire were visible 15 minutes after turning on the electric field. To visualize vesicles detached from the wire, the lipids were hydrated with a 200 mOsM sucrose solution. After applying the electric field for 45 minutes, 25 µl of the vesicle solution was diluted in 100 µl of a 200 mOsM glucose solution on a cover slide where the vesicles sunk to the bottom of the solution and could be visualized.

Confocal microscopy (Olympus FluoView FV1000) was used to inspect the vesicles using a 633 nm laser and 40X water objective lens. Pore formation was induced using a 405 nm laser pulse with a power of 660 µW. Laser irradiation spot size and irradiation time were chosen based on the noted laser fluence in the text. Z-stack slices were obtained using a 0.4 µm step size and reconstructed into a 3D image using ImageJ (National Institutes of Health). For all experiments requiring the loading or release of molecules, GPVs were formed for 2 hours prior to addition of fluorophores or manipulation of GPVs. For fluorophore diffusion into the GPVs, carboxyfluorescein (81002, AnaSpec Inc.), Texas Red dextran (MW 10 000 Da, D-1828, Invitrogen) and TRITC dextran (MW 155 000 Da,T1287, Sigma-Aldrich) were added to the medium and observed using a 488nm laser for carboxyfluorescein and 543 nm for both Texas Red dextran and TRITC dextran. For release of cargo from GPVs, vesicles were formed in the presence of TRITC-dextran (155 kDa) and carboxyfluorescein (0.4 kDa). GPVs were washed with 2 ml of 2 mM Tris pH8 using a syringe pump to replace the buffer containing fluorescent molecules exterior to the GPVs. A low flow rate (6ml/hr) was used in order to not disturb the GPVs attached to the wire. GPVs were then irradiated with low or high laser fluence as indicated in the text. Diffusion equilibrium was quantified by normalizing the fluorescence inside the GPV to the initial fluorescence outside of the GPV as a function of time using ImageJ.

For controlled DNA fluorescence and quenching, an oligonucleotide with the sequence GGTTTTGTTGTTGTTGTTTTC-Fluorescein (Sigma) was added to the external medium at 1 µM concentration with 1 mM NaCl. After performing light induced loading, the complementary sequence DAB-GAAAACAACAACAACAAAACC (Sigma) was added to the external medium in a ten fold excess and GPV opening was repeated.

For avidin-biotin binding, 70% porphyrin-lipid GPVs were formed with 0.05% DSPE-Biotin (Avanti Polar Lipids) by depositing eight 1 µl droplets of 0.5 mg/ml on the wires and rehydrating with water. Once formed, 2 mM Tris pH8 was added with 12 nM avidin (AVD407, BioShop Canada Inc.) to the external medium to block the biotin binding sites on the outer leaf of the GPV. After 15 minutes, 24 nM fluorescein conjugated avidin (APA011F, BioShop Canada Inc.) was added to the buffer and the GPV was opened several times to observe fluorescent avidin binding to the biotin binding sites on the inner leaflet of the GPV.

For physiological conditions, GPVs were formed in phosphate buffered saline under a 5 V, 500 Hz AC field for 2 hours. 155 kDa TRITC dextran was added to the well and GPVs were irradiated using a laser fluence of 40 µJ/µm^2.

Supporting Information

Supporting Information is available from the Wiley Online Library or from the author.

Acknowledgements

We thank Dr. Ana Garcia-Saez for helpful discussion and guidance regarding the physics of lipidic pores. This work was supported by the Natural Sciences & Engineering Research Council of Canada, the Canadian Cancer Society, the Canadian Institute of Health Research, the Canadian Foundation of Innovation, the Princess Margaret Hospital Foundation, and the Joey and Toby Tanenbaum/ Brazilian Ball Chair in Prostate Cancer Research.

[1] K. Kurihara, M. Tamura, K. Shohda, T. Toyota, K. Suzuki, T. Sugawara, *Nature Chem.* **2011**, *3*, 775.
[2] S. S. Mansy, J. P. Schrum, M. Krishnamurthy, S. Tobe, D. A. Treco, J. W. Szostak, *Nature* **2008**, *3*, 122.
[3] P. L. Luisi, Walde, P., T. Oberholzer, *Curr. Opin. Colloid Interface Sci.* **1999**, *3*, 33.

DOI: 10.1002/smll.201302424

[4] D. Hanahan, *J. Mol. Biol.* **1983**, *3*, 557.
[5] E. Neumann, K. Rosenheck, *J. Membr. Biol.* **1972**, *3*, 279.
[6] M. Karlsson, K. Nolkrantz, M. J. Davidson, A. Stromberg, F. Ryttsen, B. Akerman, O. Orwar, *Anal. Chem.* **2000**, *3*, 5857.
[7] B. B. Praveen, D. J. Stevenson, M. Antkowiak, K. Dholakia, F. J. Gunn-Moore, *J. Biophotonics* **2011**, *3*, 229.
[8] U. K. Tirlapur, K. Konig, *Nature* **2002**, *3*, 290.
[9] A. P. Rudhall, M. Antkowiak, X. Tsampoula, M. Mazilu, N. K. Metzger, F. Gunn-Moore, K. Dholakia, *Sci. Rep.* **2012**, *3*, 858.
[10] J. F. Lovell, C. S. Jin, E. Huynh, H. Jin, C. Kim, J. L. Rubinstein, W. C. Chan, W. Cao, L. V. Wang, G. Zheng, *Nat. Mater.* **2011**, *3*, 324.
[11] M. I. Angelova, S. Soléau, P. Méléard, F. Faucon, P. Bothorel, *Trends in Colloid and Interface Science* **1992**, *3*, 127.
[12] a) E. A. Reits, J. J. Neefjes, *Nat. Cell. Biol.* **2001**, *3*, E145; b) B. L. Sprague, R. L. Pego, D. A. Stavreva, J. G. McNally, *Biophys. J.* **2004**, *3*, 3473; c) M. Edidin, Y. Zagyansky, T. J. Lardner, *Science* **1976**, *3*, 466; d) D. Axelrod, P. Ravdin, D. E. Koppel, J. Schlessinger, W. W. Webb, E. L. Elson, T. R. Podleski, *Proc. Natl. Acad. Sci. U. S. A.* **1976**, *3*, 4594.
[13] F. Brochard-Wyart, de Gennes, P.G., O. Sandre, *Phys. A.* **2000**, *3*, 32.
[14] a) E. Karatekin, O. Sandre, F. Brochard-Wyart, *Polym. Int.* **2003**, *3*, 486; b) O. Sandre, L. Moreaux, F. Brochard-Wyart, *Proc. Natl. Acad. Sci. U. S. A.* **1999**, *3*, 10591.
[15] T. Portet, R. Dimova, *Biophys. J.* **2010**, *3*, 3264.
[16] J. F. Lovell, J. Chen, M. T. Jarvi, W. G. Cao, A. D. Allen, Y. Liu, T. T. Tidwell, B. C. Wilson, G. Zheng, *J. Phys. Chem. B* **2009**, *3*, 3203.
[17] K. A. Riske, T. P. Sudbrack, N. L. Archilha, A. F. Uchoa, A. P. Schroder, C. M. Marques, M. S. Baptista, R. Itri, *Biophys. J.* **2009**, *3*, 1362.
[18] W. Caetano, P. S. Haddad, R. Itri, D. Severino, V. C. Vieira, M. S. Baptista, A. P. Schroder, C. M. Marques, *Langmuir* **2007**, *3*, 1307.
[19] E. Y. Hleb, D. O. Lapotko, *Nanotechnology* **2008**, *3*, 355702.
[20] L. J. Anderson, E. Hansen, E. Y. Lukianova-Hleb, J. H. Hafner, D. O. Lapotko, *J. Controlled Release* **2010**, *3*, 151.
[21] A. Vogel, J. Noack, G. Hüttman, G. Paltauf, *Appl. Phys.* B: Lasers Opt. **2005**, *81*, 1015.
[22] L. Paterson, B. Agate, M. Comrie, R. Ferguson, T. Lake, J. Morris, A. Carruthers, C. T. Brown, W. Sibbett, P. Bryant, F. Gunn-Moore, A. Riches, K. Dholakia, *Opt. Express* **2005**, *3*, 595.
[23] M. W. Berns, *Nature* **1972**, *3*, 483;R. L. Amy, R. Storb, *Science* **1965**, *3*, 756.
[24] M. W. Berns, W. K. Cheng, A. D. Floyd, Y. Onuki, *Science* **1971**, *3*, 903.
[25] A. Diguet, M. Yanagisawa, Y. J. Liu, E. Brun, S. Abadie, S. Rudiuk, D. Baigl, *J. Am. Chem. Soc.* **2012**, *3*, 4898.
[26] J. F. Lovell, C. S. Jin, E. Huynh, T. D. MacDonald, W. Cao, G. Zheng, *Angew. Chem.* **2012**, *3*, 2429.

Received: August 7, 2013
Revised: October 9, 2013
Published online:

DOI: 10.1002/smll.201302424